Hindawi
International Journal of Mathematics and Mathematical Sciences
Volume 2023, Article ID 2831846, 14 pages
https://doi.org/10.1155/2023/2831846

Research Article

Analysis of Turberculosis-COVID-19 Coinfection Using Fractional Derivatives

Samuel Okyere,[1] **Joseph Ackora-Prah**,[1] **Saleem Abdullah**,[2] **Samuel Akwasi Adarkwa**,[3] **Frank Kofi Owusu**,[3] **Kwame Bonsu**,[4] **Mary Osei Fokuo**,[1] **and Mary Ann Yeboah**[3]

[1]*Department of Mathematics, Kwame Nkrumah University of Science and Technology, Kumasi, Ghana*
[2]*Department of Mathematics, Abdul Wali Khan University, Mardan, Khyber Pakhtunkhwa, Pakistan*
[3]*Department of Statistical Sciences, Kumasi Technical University, Kumasi, Ghana*
[4]*Department of Mathematics, Sunyani Technical University, Sunyani, Ghana*

Correspondence should be addressed to Samuel Okyere; okyere2015@gmail.com

Received 9 August 2022; Revised 12 November 2022; Accepted 15 April 2023; Published 24 April 2023

Academic Editor: Remi Léandre

Fractional-order derivative modeling continues to receive great interest among researchers across the globe. In this study, Tuberculosis-COVID-19 coinfection is studied using Atangana–Baleanu fractional-order derivatives defined in Caputo sense. We confirmed the existence and singularity of the solution and investigated the model's equilibrium points. Additionally, we examined the model's stability in terms of the Ulam–Hyers and generalized Ulam–Hyers stability criteria. The basic reproduction number R_0 was calculated using the next-generation matrix approach. We also looked into the model's disease-free equilibrium point's regional stability. Numerical scheme for simulating the fractional-order system with Mittag–Leffler Kernels are presented. Numerical simulations are given to validate the model. Results of the simulation showed a decline in the number of COVID-19 infections within the population when the fractional operator was reduced.

1. Introduction

A viral pneumonia-like sickness known as COVID-19, which is still a pandemic, first appeared in Wuhan, China, in December 2019, and it has since spread to 230 other countries [1, 2]. As of 23rd July 2022, there had been 574,241,843 confirmed cases and 6,401,850 fatalities as a result of the disease [3]. The effects of COVID-19 on the health of persons with underlying health issues such as cancer, cerebrovascular disease, heart failure, coronary artery disease, cardiomyopathies, diabetes mellitus, tuberculosis, and hypertension are now well established [4].

A bacterial infection called tuberculosis (TB) is contracted by breathing microscopic droplets from an infected person's cough or sneeze. Although the stomach (abdomen), glands, bones, and neurological system can also be harmed, the lungs are the organs most commonly affected [5]. In 2018, 1.7 billion people, or over 23 percent of the world's population, were infected with tuberculosis. The most lethal infectious illness in the world is tuberculosis, which claims 1.5 million lives per year. A TB bacteria infection does not always result in illness. Latent tuberculosis infection (LTBI) and TB disease are as a result two TB-related conditions. TB infection can be fatal if not properly treated. Research conducted by [6] indicates that TB causes 13% of COVID-19 fatalities.

The dynamics of the spread of the disease can be studied using the framework provided by the works in [7], although there is currently little study on the modeling of TB and COVID-19 coinfection. This study suggests using fractional-order derivatives to investigate how COVID-19 and tuberculosis are transmitted. Worldwide, academics' interest in fractional-order derivative modeling is still very high [7–18]. Leibniz believed fractional calculus to be a paradox, yet it has since developed into a topic of interest for numerous scholars from a variety of fields. As a result, several novel concepts had been developed, leading to significant divisions in the past with regard to fractional calculus [19].

Fractional-order derivatives have been used to model diseases such as measles [20], tuberculosis [21], HIV/AIDS [17, 22], polio [18] and many more. A fractional-order differential equation model in the Caputo sense was proposed by Lichae et al. [22] to explore the HIV-1 infection of CD4+ T-cells and the impact of medication therapy. Using the fractional operators Caputo and the Atangana–Baleanu, authors in [21] created a unique fractional model to examine the dynamics of the tuberculosis model with two age groups of humans, namely, children and adults. The Atangana–Baleanu fractional derivative, which has its formulation based on the renowned Mittag–Leffler kernel, was used by Karaagac and Owalabi [18] in place of the conventional polio model.

In some recent investigations, this fatal COVID-19 epidemic was mathematically modeled utilizing some of these practical derivative operators [23–29]. Using the fractional operators Caputo and the Atangana–Baleanu, authors in [24], formulated a fractional-order SEIRD model to study the spread of the disease in Italy. In order to analyze the dynamics of the COVID-19 outbreak in Pakistan, Aba Oud et al. [25] developed a fractional epidemic model in the Caputo sense that took quarantine, isolation, and environmental effects into account. To investigate the COVID-19 epidemic in Nigeria, the authors of [26] formulated an autonomous nonlinear Atangana–Baleanu fractional-order differential equation model. A nonlinear COVID-19 epidemiological model of the Caputo type was suggested by Ullah et al. [27] to investigate the importance of lockdown dynamics in restricting the transmission of infectious disease. To study the novel coronavirus outbreak, Mekonen et al. [28] suggested an SEIQRDP fractional-order deterministic model defined by Caputo derivative. In [29], a new nonlinear SEIQR fractional-order pandemic model for the Coronavirus disease (COVID-19) with Atangana–Baleanu derivative was formulated.

It has been established that the memory effects are connected to fractional-order, making it more useful for modeling epidemic diseases [24]. Based on the literature's existing COVID-19 and TB studies, we recreated the work in [7] using a fractional-order derivatives defined in Atangana–Baleanu in Caputo sense. The dynamics of the TB-COVID-19 coinfection disease are poorly represented by the classical model proposed in [7], which falls short of best portraying nonlocal behaviour. The Atangana–Baleanu and Caputo derivatives, have a number of desirable properties, such as a nonlocal and nonsingular kernel, which allows a better explanation of the crossover behaviour in the model. The other operators, such as Caputo and Caputo-Fabrizio, which lack these characteristics, may or may not be able to adequately characterize the dynamics of the cormobidity model. To the best of our knowledge, Modeling TB-COVID-19 using the Atangana–Baleanu and Caputo fractional derivatives has never been explored.

Afterwards, the article is divided into the following sections: In Section 2, we designed and investigated a mathematical model utilizing the fractional-order derivative defined in the Caputo meaning of Atangana–Baleanu, and then we presented a few definitions in fractional calculus. Additionally, we talked about the model's stability analysis in the context of Ulam–Hyers and generalized Ulam–Hyers stability criteria. We identified the qualitative characteristics of the model in Section 3. Using the next-generation method, we calculated the fundamental reproduction number. As in [7], we ascertained the equilibrium points and stability of the disease-free equilibrium point. A numerical scheme for the fractional-order model is implemented in Section 4. The numerical simulation of the model is covered in Section 5 of the study. We looked into how the different compartments are affected by the fractional-order operator. Finally, we examined and summarized the findings of our developed fractional-order model in Section 6.

2. Model Formulation

In this section, we used fractional derivatives defined in the senses of Atangana–Baleanu and Caputo to improve the TB and COVID-19 comorbidity model provided in [7]. The population comprises of eight (8) mutually exclusive classes, namely, susceptible individuals $S(t)$, latent TB infected individuals $L_T(t)$, active TB infected individuals $I_T(t)$, COVID-19 asymptomatic individuals $I_A(t)$, COVID-19 symptomatic individuals I_S, latent TB and COVID-19 coinfected individuals $L_{TC}(t)$, active TB and COVID-19 coinfected individuals I_{TC}, and recovered population from both TB and COVID-19 $R(t)$. We considered all the assumptions in [7]. We defined the fractional-order operator as b, where $0 < b \leq 1$. The schematic diagram of the model is given in Figure 1.

The following fractional derivatives describe the following model:

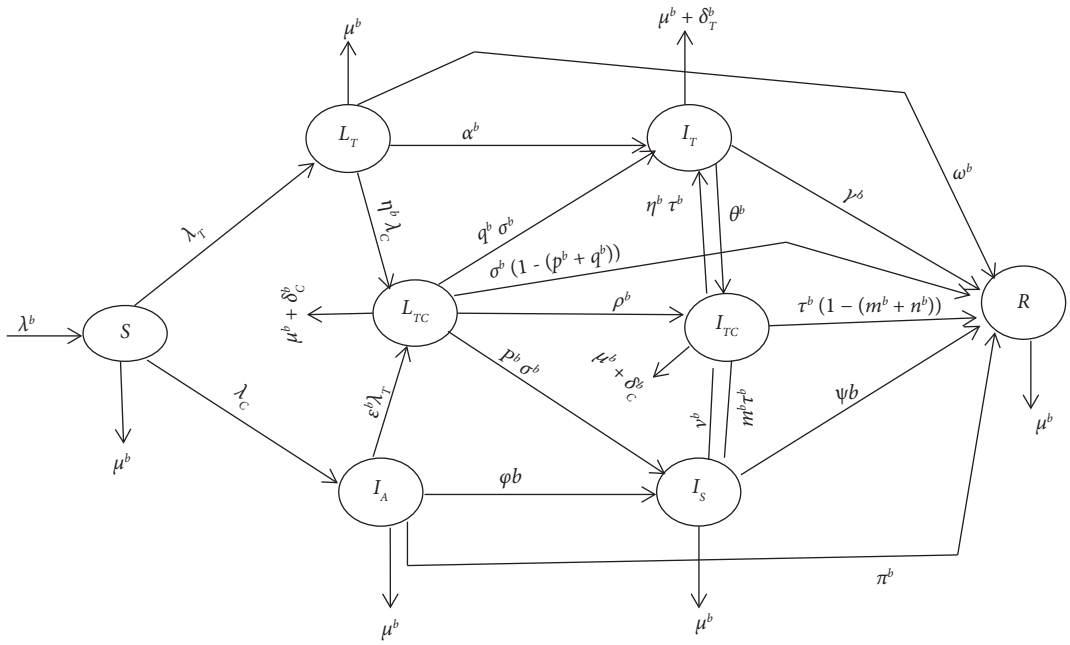

Figure 1: Schematic diagram of the tuberculosis-COVID-19 model.

$$
\begin{aligned}
{}_b^{ABC}D_t^b S &= \lambda^b - \left(\lambda_T + \lambda_C + \mu^b\right)S,\\
{}_b^{ABC}D_t^b L_T &= \lambda_T S - \left(\mu^b + \alpha^b + \eta^b\lambda_C + \omega^b\right)L_T,\\
{}_b^{ABC}D_t^b I_T &= \alpha^b L_T + q^b\sigma^b L_{TC} + n^b\tau^b I_{TC} - \left(\delta_T^b + \gamma^b + \mu^b + \theta^b\right)I_T,\\
{}_b^{ABC}D_t^b I_A &= \lambda_C S - \left(\varphi^b + \epsilon^b\lambda_T + \pi^b + \mu^b\right)I_A,\\
{}_b^{ABC}D_t^b I_S &= \varphi^b I_A + p^b\sigma^b L_{TC} + m^b\tau^b I_{TC} - \left(\nu^b + \mu^b + \delta_C^b + \psi^b\right)I_S,\\
{}_b^{ABC}D_t^b L_{TC} &= \eta^b\lambda_C L_T + \epsilon^b\lambda_T I_A - \left(\delta_C^b + \rho^b + \mu^b + \sigma^b\right)L_{TC},\\
{}_b^{ABC}D_t^b I_{TC} &= \rho^b L_{TC} + \theta^b I_T + \nu^b I_S - \left(\mu^b + \delta_{TC}^b + \tau^b\right)I_{TC},\\
{}_b^{ABC}D_t^b R &= \omega^b L_T + \pi^b I_A + \gamma^b I_T + \psi^b I_S + \sigma^b\left(1 - \left(p^b + q^b\right)\right)L_{TC} + \left(1 - \left(m^b + n^b\right)\right)\tau^b I_{TC} - \mu^b R,
\end{aligned}
\tag{1}
$$

with force of infection

$$
\lambda_T(t) = \beta_1^b\left(\frac{I_T(t) + I_{TC}(t)}{N(t)}\right), \lambda_C(t) = \beta_2^b\left(\frac{I_A(t) + I_S(t) + L_{TC}(t) + I_{TC}(t)}{N(t)}\right), \tag{2}
$$

and non-negativity initial conditions $S(0) \geq 0, L_T(0) \geq 0, I_T(0) \geq 0, I_A(0) \geq 0, I_S(0) \geq 0, \quad L_{TC}(0) \geq 0, I_{TC} \geq 0,$ and $R(0) \geq 0$. The parameter and description are given in Table 1.

2.1. Preliminaries. In this section, we reviewed the fundamental definitions of fractional calculus that were provided in [8] and were applied in this work.

Definition 1. The fractional derivative of order b is defined by Liouville and Caputo (LC) in [8, 11, 30] as follows:

$$
\begin{aligned}
{}_b^C D_t^b h(t) &= \frac{1}{\Gamma(1-b)}\int_0^t (t-p)^{-b}\dot{h}(p)\mathrm{d}p, 0 < b \leq 1,\\
\frac{\partial h(p)}{\partial t} &= \dot{h}(p), b = 1.
\end{aligned}
\tag{3}
$$

Table 1: Parameter and description.

Parameter	Description
λ	Recruitment rate
β_2	Transmission rate of COVID-19
β_1	Transmission rate of TB disease
α	The rate at which latent TB infected individuals becomes active TB
φ	The rate at which asymptomatic individuals becomes symptomatic
μ	Natural death rate
δ_T	Death rate due to TB disease
δ_C	Disease-induced death rate of COVID-19
θ	COVID-19 infection rate from the TB infected individuals
π	Recovery rate of asymptomatic individuals
ψ	Recovery rate of symptomatic individuals
σ	The rate at which individuals leave the L_{TC} compartment
γ	The recovery rate of TB infected individuals
τ	The rate at which individuals move from the coinfected class
ρ	Transfer rate of latent TB-COVID-19 patients to coinfected TB-COVID-19
η	Rate at which latent TB individuals contract COVID-19
ϵ	The rate at which asymptomatic individuals become exposed to TB
ν	Disease-induced death rate
ω	Recovery rate of TB latent infected individuals
n	Recovery rate of I_{TC} individuals from COVID-19
m	Recovery rate of I_{TC} individuals from COVID-19
p	Recovery rate of L_{TC} individuals from COVID-19
q	Recovery rate of L_{TC} individuals from TB

Definition 2. The Liouville–Caputo sense definition of the Atangana–Baleanu fractional derivative is given in [8, 9].

$$ {}_{b}^{ABC}D_t^b h(t) = \frac{B(b)}{(1-b)} \int_0^t E_b\left(-b\left(\frac{(t-p)^b}{1-b}\right)\right)\dot{h}(p)\mathrm{d}p, \tag{4} $$

where $B(b) = 1 - b + b/\Gamma(b)$ is the normalized function.

Definition 3. Regarding the Atangana–Baleanu–Caputo derivative, the relevant fractional integral is defined as follows [8]:

$$ {}_{b}^{ABC}I_t^b h(t) = \frac{(1-b)}{B(b)} h(t) + \frac{b}{B(b)\Gamma(b)} \int_0^t (t-p)^{b-1} h(p)\mathrm{d}p. \tag{5} $$

They computed the Laplace transform of both derivatives and obtained the following equation [15]:

$$ L\left\{{}_{0}^{ABC}D_t^b h(t)\right\} = \frac{B(b)H(q)q^b - q^{b-1}h(0)}{(1-b)\left(q^b + b/1-b\right)}. \tag{6} $$

where L is the Laplace transform operator.

Theorem 1. *For a function $h \in C[a,b]$, the following results holds [8, 12]: $\|{}_{b}^{ABC}D_t^b r(t)\| < B(b)/(1-b)\|h(t)\|$, where $\|h(t)\| = \max_{a\le t\le b}|h(t)|$.*

Furthermore, the Atangana–Baleanu–Caputo derivatives fulfil the following Lipschitz condition [8, 12]:

$$ \left\|{}_{b}^{ABC}D_{,t}^b h_1(t) - {}_{b}^{ABC}D_t^b h_2(t)\right\| < \omega\left\|h_1(t) - h_2(t)\right\|. \tag{7} $$

2.2. Hyers–Ulam Stability

Definition 4. Equation (1)'s ABC fractional system is considered to be Hyers–Ulam stable if for every $\Phi_i > 0, i \in N^k$ there exists constants $\lambda_i > 0, i \in N^k$ satisfying the following equation:

$$ \left|F(t) - \frac{1-b}{B(b)}\Phi_i(b,t,F(t)) + \frac{b}{B(b)\Gamma(b)} \times \int_0^t (t-\varsigma)^{b-1}\Phi_i(b,\varsigma,F(\tau))\mathrm{d}\tau\right| \le \lambda_i, \tag{8} $$

and there exist $\dot{F}(t)$ where

$$\dot{F}(t) = \frac{1-b}{B(b)}\Phi_i(b, F(t)) + \frac{b}{B(b)\Gamma(b)} \times \int_0^t (t-\varsigma)^{b-1}\Phi_i(b, \varsigma, \dot{F}(\varsigma))\mathrm{d}\varsigma, \tag{9}$$

such that

$$|F(t) - \dot{F}(t)| \leq \xi_i \lambda_i. \tag{10}$$

Now considering the system (1), we have the following equation:

$$\begin{aligned}
&\left|S(t) - \frac{1-b}{B(b)}\Phi_1(b, t, S(t)) + \frac{b}{B(b)\Gamma(b)} \times \int_0^t (t-\varsigma)^{b-1}\Phi_1(b, \varsigma, S(\tau))\mathrm{d}\tau\right| \leq \lambda_1,\\
&\left|L_T(t) - \frac{1-b}{B(b)}\Phi_2(b, t, L_T(t)) + \frac{b}{B(b)\Gamma(b)} \times \int_0^t (t-\varsigma)^{b-1}\Phi_2(b, \varsigma, L(\tau))\mathrm{d}\tau\right| \leq \lambda_2,\\
&\left|I_T(t) - \frac{1-b}{B(b)}\Phi_3(b, t, I_T(t)) + \frac{b}{B(b)\Gamma(b)} \times \int_0^t (t-\varsigma)^{b-1}\Phi_3(b, \varsigma, I_T(\tau))\mathrm{d}\tau\right| \leq \lambda_3,\\
&\left|I_A(t) - \frac{1-b}{B(b)}\Phi_4(b, t, I_A(t)) + \frac{b}{B(b)\Gamma(b)} \times \int_0^t (t-\varsigma)^{b-1}\Phi_4(b, \varsigma, I_A(\tau))\mathrm{d}\tau\right| \leq \lambda_4,\\
&\left|I_S(t) - \frac{1-b}{B(b)}\Phi_5(b, t, I_S(t)) + \frac{b}{B(b)\Gamma(b)} \times \int_0^t (t-\varsigma)^{b-1}\Phi_5(b, \varsigma, I_S(\tau))\mathrm{d}\tau\right| \leq \lambda_5,\\
&\left|L_{TC}(t) - \frac{1-b}{B(b)}\Phi_6(b, t, L_{TC}(t)) + \frac{b}{B(b)\Gamma(b)} \times \int_0^t (t-\varsigma)^{b-1}\Phi_6(b, \varsigma, L_{TC}(\tau))\mathrm{d}\tau\right| \leq \lambda_6,\\
&\left|I_{TC}(t) - \frac{1-b}{B(b)}\Phi_7(b, t, I_{TC}(t)) + \frac{b}{B(b)\Gamma(b)} \times \int_0^t (t-\varsigma)^{b-1}\Phi_7(b, \varsigma, I_{TC}(\tau))\mathrm{d}\tau\right| \leq \lambda_7,\\
&\left|R(t) - \frac{1-b}{B(b)}\Phi_8(b, t, R(t)) + \frac{b}{B(b)\Gamma(b)} \times \int_0^t (t-\varsigma)^{b-1}\Phi_8(b, \varsigma, R(\tau))\mathrm{d}\tau\right| \leq \lambda_8,
\end{aligned} \tag{11}$$

and there exist $\left\{\dot{S}(t), \dot{L}_T(t), \dot{I}_T(t), \dot{I}_A(t), \dot{I}_S(t), \dot{L}_{TC}(t), \dot{I}_{TC}(t), \dot{R}(t)\right\}$, where

$$
\begin{aligned}
\overset{\bullet}{S}(t) &= \frac{1-b}{B(b)}\Phi_1(b,t,S(t)) + \frac{b}{B(b)\Gamma(b)} \times \int_0^t (t-\tau)^{b-1}\Phi_1(b,\tau,\overset{\bullet}{S}(\tau))\mathrm{d}\tau,\\
\bullet L_T(t) &= \frac{1-b}{B(b)}\Phi_2(b,t,L_T(t)) + \frac{b}{B(b)\Gamma(b)} \times \int_0^t (t-\tau)^{b-1}\Phi_2(b,\tau,\overset{\bullet}{L}(\tau))d\tau,\\
\bullet I_T(t) &= \frac{1-b}{B(b)}\Phi_3(b,t,I_T(t)) + \frac{b}{B(b)\Gamma(b)} \times \int_0^t (t-\tau)^{b-1}\Phi_3\left(b,\tau,\overset{\bullet}{I}_T(\tau)\right)\mathrm{d}\tau,\\
\bullet I_A(t) &= \frac{1-b}{B(b)}\Phi_4(b,t,I_A(t)) + \frac{b}{B(b)\Gamma(b)} \times \int_0^t (t-\tau)^{b-1}\Phi_4\left(b,\tau,\overset{\bullet}{I}_A(\tau)\right)\mathrm{d}\tau,\\
\bullet I_S(t) &= \frac{1-b}{B(b)}\Phi_5(b,t,Q(t)) + \frac{b}{B(b)\Gamma(b)} \times \int_0^t (t-\tau)^{b-1}\Phi_3(b,\tau,\bullet I_S(\tau))\mathrm{d}\tau,\\
\bullet L_{TC}(t) &= \frac{1-b}{B(b)}\Phi_6(b,t,L_{TC}(t)) + \frac{b}{B(b)\Gamma(b)} \times \int_0^t (t-\tau)^{b-1}\Phi_6(b,\tau,\bullet L_{TC}(\tau))\mathrm{d}\tau,\\
\bullet I_{TC}(t) &= \frac{1-b}{B(b)}\Phi_7(b,t,I_{TC}(t)) + \frac{b}{B(b)\Gamma(b)} \times \int_0^t (t-\tau)^{b-1}\Phi_7(b,\tau,\bullet I_{TC}(\tau))\mathrm{d}\tau,\\
\overset{\bullet}{R}(t) &= \frac{1-b}{B(b)}\Phi_8(b,t,R(t)) + \frac{b}{B(b)\Gamma(b)} \times \int_0^t (t-\tau)^{b-1}\Phi_8(b,\tau,\overset{\bullet}{R}(\tau))\mathrm{d}\tau,
\end{aligned}
\tag{12}
$$

such that

$$
\begin{aligned}
&|S(t)-\overset{\bullet}{S}(t)| \le \xi_1\lambda_1, \left|L_T(t)-\bullet L_T(t)\right| \le \xi_2\lambda_2, \left|I_T(t)-\bullet I_T(t)\right| \le \xi_3\lambda_3, \left|I_A(t)-\bullet I_A(t)\right| \le \xi_4\lambda_4,\\
&\left|I_S(t)-\bullet I_S(t)\right| \le \xi_5\lambda_5, \left|L_{TC}(t)-\bullet L_{TC}(t)\right| \le \xi_6\lambda_6, \left|I_{TC}(t)-\bullet I_{TC}(t)\right| \le \xi_7\lambda_7, |R(t)-\overset{\bullet}{R}(t)| \le \xi_8\lambda_8.
\end{aligned}
\tag{13}
$$

3. Analysis of the Coinfection Model

The disease-free equilibrium (E_0) is the steady state solution where there is no infection in the population. This is given as follows:

$$
E_0 = \left(S^0, L_T^0, I_T^0, I_A^0, I_S^0, L_{TC}^0, I_{TC}^0, R^0\right) = \left(\frac{\lambda^b}{\mu^b}, 0, 0, 0, 0, 0, 0, 0\right).
\tag{14}
$$

The endemic equilibrium (E_1) of system (1) is $E_1 = (S^*, L_T^*, I_T^*, I_A^*, I_S^*, L_{TC}^*, I_{TC}^*, R^*)$, where

$$
\begin{aligned}
S^* &= \frac{\lambda^b}{\lambda_T+\lambda_C+\mu^b}, L_T^* = \frac{\lambda_T S^*}{\alpha^b+\eta^b\lambda_C+\mu^b+\omega^b}, I_A^* = \frac{\lambda_C S^*}{\pi^b+\mu^b+\varphi^b+\epsilon^b\lambda_T},\\
I_T^* &= \frac{\alpha L_T^* + q\sigma^b L_{TC} + n\tau^b I_{TC}^*}{\gamma^b+\mu^b+\delta_T^b+\theta^b}, I_S^* = \frac{\varphi^b L_A^* + p\sigma^b L_{TC}^* + m\tau^b I_{TC}^*}{\beta g A^* + \left(\nu^b+\mu^b+\varphi^b+\delta_C^b\right)},\\
L_{TC}^* &= \frac{\eta^b\lambda_C L_T^* + \epsilon Q^*}{\mu},\\
I_{TC}^* &= \frac{\rho^b L_{TC}^* + \theta^b I_T^* + \nu^b I_S^*}{\left(\mu^b+\delta_{TC}^b+\tau^b\right)},\\
R^* &= \frac{\omega^b L_T^* + \pi^b I_A^* + \gamma^b I_T^* + \psi^b I_S^* + \sigma^b\left(1-\left(p^b+q^b\right)\right)L_{TC}^* + \left(1-\left(m^b+n^b\right)\right)\tau^b I_{TC}^*}{\mu^b}.
\end{aligned}
\tag{15}
$$

We now determine the system's basic reproduction number which is the total number of secondary cases that can be produced by a single infected person over the course of an illness in a population that is completely susceptible [14]. Denote F and V, respectively, as matrices for the newly created diseases and the transition terms we found using the next-generation operator approach [14].

$$F = \begin{bmatrix} 0 & \beta_1^b & 0 & 0 & 0 & \beta_1^b \\ 0 & 0 & 0 & 0 & 0 & 0 \\ 0 & 0 & \beta_2^b & \beta_2^b & \beta_2^b & \beta_2^b \\ 0 & 0 & 0 & 0 & 0 & 0 \\ 0 & 0 & 0 & 0 & 0 & 0 \\ 0 & 0 & 0 & 0 & 0 & 0 \end{bmatrix},$$
$$V = \begin{bmatrix} A_1 & 0 & 0 & 0 & 0 & 0 \\ -\alpha^b & A_2 & 0 & 0 & -q\sigma^b & -n\tau^b \\ 0 & 0 & A_3 & 0 & 0 & 0 \\ 0 & 0 & -\varphi & A_4 & -p\sigma & -m\tau^b \\ 0 & 0 & 0 & 0 & A_5 & 0 \\ 0 & -\theta^b & 0 & -\nu & 0 & A_6 \end{bmatrix}, \tag{16}$$

where $A_1 = \mu^b + \alpha^b + \omega^b$, $A_2 = \mu^b + \theta^b + \delta_T{}^b + \gamma^b$, $A_3 = \mu^b + \varphi^b + \pi^b A_4 = \mu^b + \nu + \delta_C^b + \psi^b$, $A_5 = \mu^b + \delta_C^b + \rho^b + \sigma^b$, and $A_6 = \mu^b + \tau^b + \delta_{TC}^b$

The basic reproduction number is the largest eigenvalue of the next-generation matrix FV^{-1} given by the following equation:

$$R_0 = \max\left\{\left|R_1\right|, \left|R_2\right|\right\}, \tag{17}$$

where

$$R_1 = \frac{A_1 J_4 + \alpha^b A_3 J_1 - \sqrt{\alpha^b A_3^2 J_1^2 - 2\alpha^b A_1 A_3 J_1 J_3 + 4\varphi^b \alpha^b A_1 A_3 J_2^2 + A_1^2 J_4^2}}{2A_1 A_2 A_3 m\nu^b \tau^b + A_4\left(n\theta^b \tau^b - A_2 A_6\right)},$$
$$R_2 = \frac{A_1 J_4 + \alpha^b A_3 J_1 + \sqrt{\alpha^b A_3^2 J_1^2 - 2\alpha^b A_1 A_3 J_1 J_3 + 4\varphi^b \alpha^b A_1 A_3 J_2^2 + A_1^2 J_4^2}}{2A_1 A_2 A_3 m\nu^b \tau^b + A_4\left(n\theta^b \tau^b - A_2 A_6\right)}, \tag{18}$$

where

$$\begin{aligned} J_1 &= -\beta_1^b\left(A_4 A_6 + \theta^b A_4 - m\nu^b \tau^b\right), J_2 = -\beta_2^b \theta^b\left(A_4 + m\tau^b\right), J_3 = -\beta_1^b \nu^b\left(A_2 + n\tau^b\right), \\ J_4 &= -\beta_2^b A_2\left(A_4 A_6 + \varphi^b A_6 + \nu^b \varphi^b - m\nu^b \tau^b\right) - n\theta^b \tau^b\left(A_4 + \varphi^b\right), \\ J_5 &= -\beta_1^b\left(\rho^b A_4\left(A_2 + \nu^b \tau^b\right) + q\sigma^b A_4\left(A_6 + \theta^b\right) + A_2 pq\nu^b + \nu^b \rho^b \tau^b (np - mq)\right), \\ J_6 &= -\beta_2^b\left(A_2 A_4\left(A_6 + \rho^b\right) + A_2 m\tau^b\left(\rho^b - \nu^b\right) + c_2 p\sigma^b\left(A_6 + \nu^b\right) + J_7\right), \\ J_7 &= q\theta^b \sigma^b\left(A_4 + m\tau^b\right) - n\theta^b \tau^b\left(A_4 + p\sigma^b\right). \end{aligned} \tag{19}$$

3.1. Local Stability of the Disease-Free Equilibrium Point. The Jacobian matrix of the system (1) evaluated at the disease-free equilibrium point is as follows:

$$J = \begin{pmatrix} -\mu^b & 0 & -\beta_1^b & -\beta_2^b & -\beta_2^b & -\beta_2^b & -\beta_1^b - \beta_2^b & 0 \\ 0 & -A_1 & \beta_1^b & 0 & 0 & 0 & \beta_1^b & 0 \\ 0 & \alpha^b & -A_2 & 0 & 0 & q\sigma^b & n\tau^b & 0 \\ 0 & 0 & 0 & \beta_2^b - A_3 & \beta_2^b & \beta_2^b & \beta_2^b & 0 \\ 0 & 0 & 0 & \varphi^b & -A_4 & p\sigma^b & m\tau^b & 0 \\ 0 & 0 & 0 & 0 & 0 & -A_5 & 0 & 0 \\ 0 & 0 & \theta^b & 0 & \nu^b & \rho^b & -A_6 & 0 \\ 0 & \omega^b & \gamma^b & \pi^b & \psi^b & (1-(p+q))\sigma^b & (1-(m+n))\tau^b & -\mu^b \end{pmatrix}. \tag{20}$$

The first three eigenvalues of system (20) can be obtained from the first and eight columns and the sixth row given as $\lambda_{1,2} = -\mu^b$ and $\lambda_3 = -A_5$. The remaining five eigenvalues are obtained from the characteristic equation of the following reduced matrix:

$$J = \begin{pmatrix} -A_1 & \beta_1^b & 0 & 0 & \beta_1^b \\ \alpha^b & -A_2 & 0 & 0 & n\tau^b \\ 0 & 0 & \beta_2^b - A_3 & \beta_2^b & \beta_2^b \\ 0 & 0 & \varphi^b & -A_4 & m\tau^b \\ 0 & \theta^b & 0 & \nu^b & -A_6 \end{pmatrix}. \tag{21}$$

The characteristic equation of system (21) is as follows:

$$\xi^5 + b_1\xi^4 + b_2\xi^3 + b_3\xi^2 + b_4\xi + b_5 = 0, \tag{22}$$

where

$$\begin{aligned} b_1 &= \left(\beta_2^b + A_2 + A_6 - A_1 - A_3 - A_4\right), \\ b_2 &= \beta_2^b\varphi^b + A_4\left(\beta_2^b - A_3\right) + p_1p_2 + \left(\alpha^b\beta_1^b + n\tau^b\theta^b - p_3\right), \\ b_3 &= \alpha^b\beta_1^b\left(A_6 + \theta^b\right) + A_1\left(n\theta\tau - A_2A_6\right) - \beta_2^b\varphi^b + p_1A_4\left(\beta_2^b - A_3\right) - p_2\left(\alpha^b\beta_1^b + n\tau^b\theta^b - p_3\right), \\ b_4 &= -\left(\beta_2^b\varphi^b + A_4\left(\beta_2^b - A_3\right)\right)\left(\alpha^b\beta_1^b + n\tau^b\theta^b - p_3\right) - p_2\left(\alpha^b\beta_1^b\left(A_6 + \theta^b\right) + A_1\left(n\theta^b\tau^b - A_2A_6\right)\right), \\ b_5 &= \left(\beta_2^b\varphi^b + A_4\left(\beta_2^b - A_3\right)\right)\left(\alpha^b\beta_1^b\left(A_6 + \theta^b\right) + A_1\left(n\theta^b\tau^b - A_2A_6\right)\right), \\ p_1 &= A_2 + A_6 - A_1, \\ p_2 &= A_3 + A_4 + \beta_2^b, \\ p_3 &= A_2A_6 + A_1\left(A_2 + A_6\right). \end{aligned} \tag{23}$$

Thus, using the Routh–Hurwitz stability criterion, the roots of characteristic (22) is stable if it satisfies the following condition:

$$\begin{aligned} b_i > 0, i = 1, 2, 3, 4, 5, \\ b_1b_2b_3 > {b_3}^2 + {b_1}^2b_4, \\ \left(b_1b_4 - b_5\right)\left(b_1b_2b_3 - {b_3}^2 - {b_1}^2b_4\right) > b_5\left(b_1b_2 - b_3\right)^2 + b_1{b_5}^2. \end{aligned} \tag{24}$$

Theorem 2. *The disease-free equilibrium point of the model is locally asymptotically stable if the condition given in equation (24) holds.*

4. Numerical Scheme of the Fractional Derivative

Let us consider the following general initial value problem:

$${}_b^{ABC}D_t^b[\zeta(t)] = r(t, \zeta(t)), \zeta(0) = \zeta_o. \tag{25}$$

Applying the fundamental theorem of fractional calculus to (25), we obtained the following equation:

$$\zeta(t)-\zeta(0)=\frac{1-b}{G(b)}h(t,\zeta(t))+\frac{b}{\Gamma(b)G(b)}\int_0^t(h(\tau,\zeta(\tau))(t-\tau)^{b-1}\mathrm{d}\varsigma, \tag{26}$$

where $G(b)=1-b+b/\Gamma(b)$ is a normalised function and at t_{x+1}, and we have the following equation:

$$\zeta_{x+1}=\zeta_o+\frac{(1-b)\Gamma(b)}{(1-b)\Gamma(b)+b}h(t_x,\zeta(t_x))+\frac{b}{\Gamma(b)+b(1-\Gamma(b))}\sum_{y=0}^{x}\int_{t_y}^{t}h\times(t_{x+1}-\varsigma)^{b-1}. \tag{27}$$

Implementing two-step Lagrange's interpolation polynomial on the interval $[t_x,t_{x+1}]$ [10], we have the following equation:

$$H=\frac{h\left(t_y,\zeta_y\right)}{u}\left(\tau-t_{y-1}\right)-\frac{h\left(t_{y-1},\zeta_{y-1}\right)}{u}\left(\tau-t_y\right). \tag{28}$$

Equation (28) is replaced with equation (24) and by performing the steps given in [9], we obtained the following equation:

$$\begin{aligned}F(t_{x+1})=F(t_0)+\frac{\Gamma(b)(1-b)}{\Gamma(b)(1-b)+b}h(t_n,\zeta(t_x))+\frac{1}{(b+1)\Gamma(b)+b}\sum_{y=0}^{x}u^b h\left(t_y,\zeta\left(t_y\right)\right)(x+1-y)^b\\ \times T-h^b h\left(t_{y-1},\zeta\left(t_{y-1}\right)\right)(x+1-y)^{b+1}(x-y+2+b)-(x-y)^b(x-y+1+b).\end{aligned} \tag{29}$$

To obtain high stability, we replaced the step size u in equation (29) with $\phi(u)$ such that $\phi(u)=u+O(u^2)$, $0<\phi(u)\le 1$ [13].

The new scheme which is called the nonstandard two–step Lagrange interpolation method (NS2LIM) is given as follows:

$$\begin{aligned}\zeta(t_{x+1})=\zeta(t_0)+\frac{\Gamma(b)(1-b)}{\Gamma(b)(1-b)+b}h(t_x,\zeta(t_x))+\frac{1}{(b+1)(1-b)\Gamma(b)+b}P\\ \times T-\varphi(h)^b h\left(t_{y-1},\zeta\left(t_{y-1}\right)\right)(x+1-y)^{b+1}(x-y+2+b)\\ -(x-y)^b(x-y+1+b),\end{aligned} \tag{30}$$

where $T=(x-y+2+b)-(x-y)^b(x-y+2+2b)$

$$P=\sum_{y=0}^{x}\varphi(u)^b h\left(t_y,\zeta\left(t_y\right)\right)(x+1-y)^b. \tag{31}$$

5. Numerical Simulation

In this study, we have replaced the time-ordinary derivative described in [7] with the time-dependent fractional-order derivatives in equation (1) and the model (1) was solved using the numerical scheme described in equation (27) using the parameter values given in Table 2 below. The initial conditions are $S(0)=10,0000, L_T=100, I_T=2, I_A=10, I_S=3, L_{TC}=3, I_{TC}=2,$ and $R=3$ [7]. Computational simulations for the proposed method of this study is performed using MATLAB and the results are displayed in Figure 2–9.

The dynamic behaviour of each compartment during a 120-day period is shown in Figures 2-9. As the fractional operator b falls from 1.0 to 0.4, the population of susceptible people shrinks. The susceptible population is found to rapidly decline and approach zero during the first 20 days of the outbreak when $b=0.4$ (see Figure 2). Figures 3 and 4 show that as the fractional operator value lowers from 1.0, the number of people with latent and active tuberculosis decreases more quickly. The number is quite small and falls to zero even before the first 10 days of the outbreak, as can be seen at $b=0.4$. Figure 5 shows that COVID-19 asymptomatic persons attain their highest peak on the tenth day at $b=0.6$ before rapidly declining. After the first 20 days and through the end of the time, the population is steady at the integer value. Additionally, it begins to degrade more quickly around $b=0.4$ and reaches zero on the tenth day.

Table 2: Parameter values.

Parameter	Value	Source
λ	500	[7]
β_2	0.659	[7, 28]
β_1	0.6	[7, 27]
α	0.25	[7, 27]
φ	0.02	[7]
μ	0.0477	[7, 28]
δ_T	0.01	[7, 27]
δ_C	0.023	[7, 28]
θ	0.001	[7]
π	0.05	[7]
ψ	0.5	[7]
σ	0.01	[7]
γ	0.516	[7]
τ	0.003	[7]
ρ	0.02	[7]
η	0.03	[7]
ϵ	0.03	[7]
ν	0.002	[7]
ω	0.09	[7, 26]

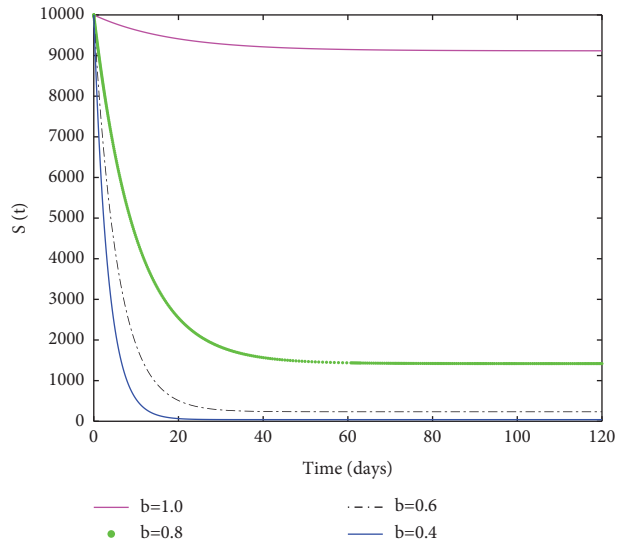

Figure 2: Behaviour of the susceptible individuals at different values of b.

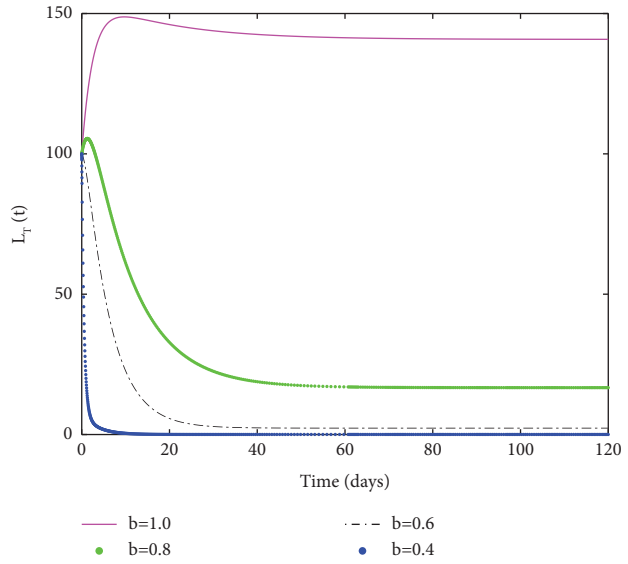

Figure 3: Behaviour of the latent TB infected individuals at different values of b.

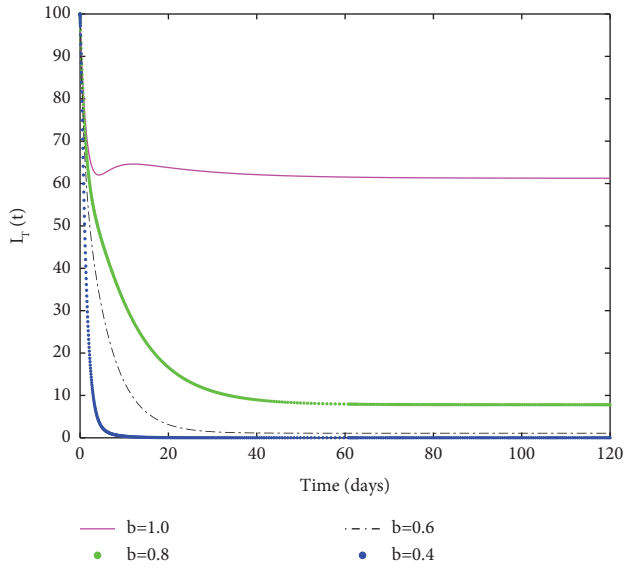

Figure 4: Behaviour of the active TB infected individuals at different values of b.

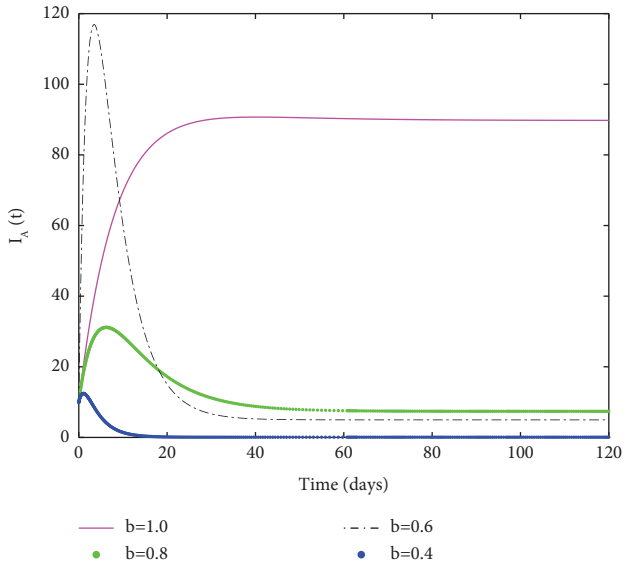

FIGURE 5: Behaviour of the COVID-19 asymptomatic individuals at different values of b.

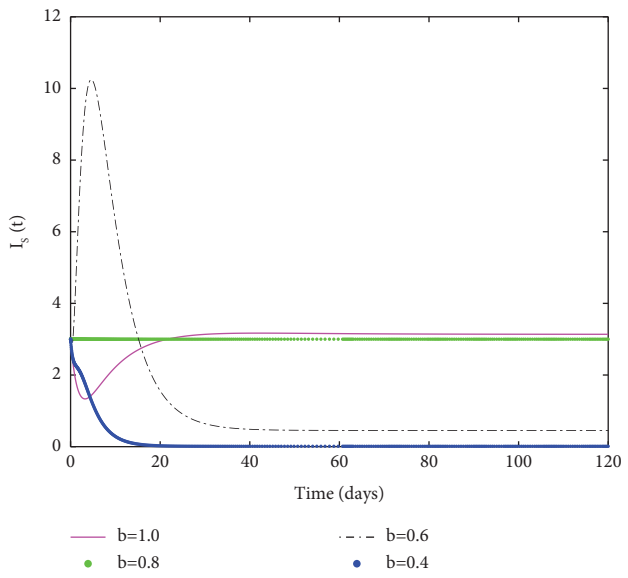

FIGURE 6: Behaviour of the COVID-19 symptomatic individuals at different values of b.

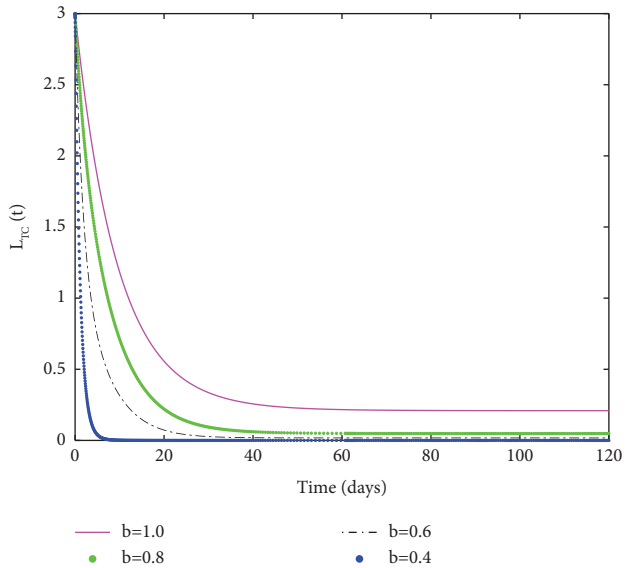

FIGURE 7: Behaviour of the latent TB-COVID-19 coinfected individuals at different values of b.

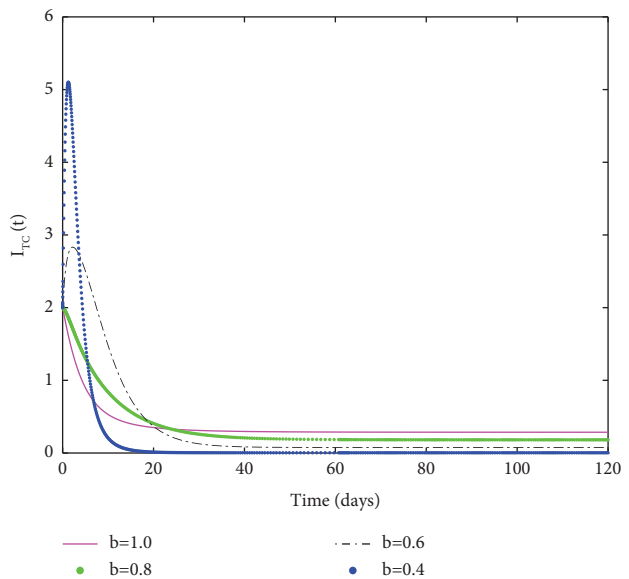

FIGURE 8: Behaviour of the active TB-COVID-19 coinfected individuals at different values of b.

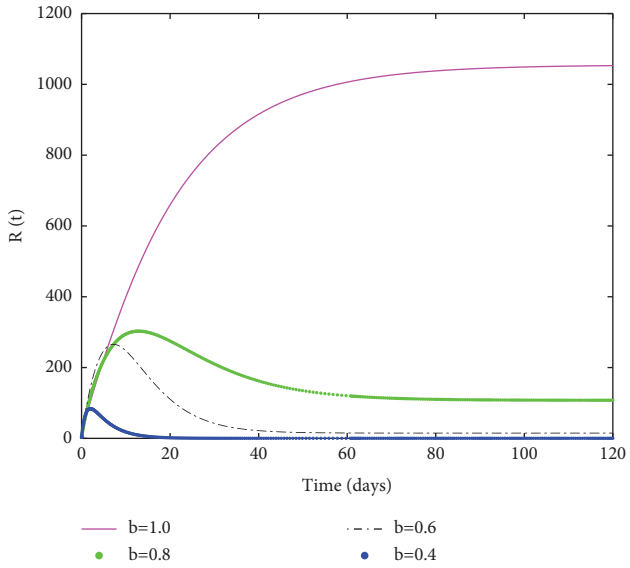

FIGURE 9: Behaviour of the recovered individuals at different values of b.

The dynamics of the COVID-19 symptomatic compartment for the first 120 days are shown in Figure 6. The population is observed to be constant across the duration at $b = 0.8$. The population becomes zero before the first 20 days at $b = 0.4$. A drop in the value of the fractional operator b from 1.0 to 0.4 has an impact on the number of people who recover from the disease as well (see Figure 9). Additionally, a decrease in the fractional operator value causes a quicker decline in the proportion of people with latent and active TB-COVID-19 coinfections (see Figures 7 and 8)

6. Conclusion

Based on the integer-order model of [7], we have presented a fractional-order epidemic model for the dynamics of the TB-COVID-19 coinfection. This study presented the qualitative analysis of the fractional-order model. We proved the asymptotic stability of the disease-free equilibrium and determined the basic reproduction number using the next-generation approach. Furthermore, we proved the uniqueness of the solution and established the stability of the model using Ulam–Hyers stability criteria. A numerical scheme for simulating the fractional-order system with Mittag–Leffler Kernels is presented. Finally, a numerical simulation was performed to validate the model. Results of the simulation showed a decline in the number of COVID-19 infections within the population when the fractional operator was reduced. The analysis of the model is far from complete. Researchers can extend this model to capture stochastic dynamics of the method used.

Data Availability

No data were used to support this study. All parameter values are duly cited and referenced.

Conflicts of Interest

The authors declare that they have no conflicts of interest.

Acknowledgments

This work was carried out at the Department of Mathematics, Kwame Nkrumah University of Science and Technology, Kumasi.

References

[1] Y. Marimuthu, B. Nagappa, N. Sharma, S. Basu, and K. K. Chopra, "COVID-19 and tuberculosis: a mathematical model based forecasting in Delhi, India," *Indian Journal of Tuberculosis*, vol. 67, no. 2, pp. 177–181, 2020.

[2] J. Hopkins, "Coronavirus Resource center," 2020, https://coronavirus.jhu.edu/data.

[3] Worldometer, "COVID-19 Coronavirus pandemic," 2022, https://www.worldometers.info/coronavirus/.

[4] Centers for Disease Control and Prevention, "Underlying medical conditions associated with higher risk for severe covid-19: information for healthcare providers," 2021, https://www.cdc.gov/coronavirus/2019-ncov/hcp/clinical-care/underlyingconditions.html.

[5] Center for Disease Control and Prevention, "Tuberculosis," 2021, https://www.cdc.gov/globalhealth/newsroom/topics/tb/index.html#::text=What%20is%20the%20global%20impact,1.5%20million%20lives%20each%20year.

[6] M. Koupaei, A. Naimi, N. Moafi et al., "Clinical characteristics, diagnosis, treatment, and mortality rate of TB/COVID-19 coinfectetd patients: a systematic review," *Frontiers of Medicine*, vol. 8, Article ID 740593, 2021.

[7] K. G. Mekonen, S. F. Balcha, L. L. Obsu, and A. Hassen, "Mathematical modeling and analysis of TB and COVID-19 coinfection," *Journal of Applied Mathematics*, vol. 2022, Article ID 2449710, 20 pages, 2022.

[8] N. H. Sweilam, S. M. Al-Mekhlafi, and D. Baleanu, "Optimal control for a fractional tuberculosis infection model including the impact of diabetes and resistant strains," *Journal of Advanced Research*, vol. 17, pp. 125–137, 2019.

[9] A. Atangana and D. Baleanu, "New fractional derivatives with non-local and non-singular kernel: theory and application to heat transfer model," *Thermal Science*, vol. 20, no. 2, pp. 763–769, 2016.

[10] J. E. Solís-Pérez, J. F. Gómez-Aguilar, and A. Atangana, "Novel numerical method for solving variable-order fractional differential equations with power, exponential and Mittag-Leffler laws," *Chaos, Solitons and Fractals*, vol. 114, pp. 175–185, 2018.

[11] B. P. Moghaddam, S. Yaghoobi, and J. T. Machado, "An extended predictor-corrector algorithm for variable-order fractional delay differential equations," *Journal of Computational and Nonlinear Dynamics*, vol. 1, pp. 1–11, 2016.

[12] C. Coll, A. Herrero, E. Sanchez, and N. Thome, "A dynamic model for a study of diabetes," *Mathematical and Computer Modelling*, vol. 50, no. 5–6, pp. 713–716, 2009.

[13] K. C. Patidar, "Nonstandard finite difference methods: recent trends and further developments," *Journal of Difference Equations and Applications*, vol. 22, no. 6, pp. 817–849, 2016.

[14] S. P. Dharmaratne, S. Sudaraka, I. Abeyagunawardena, K. Manchanayake, M. Kothalawala, and W. Gunathunga, "Estimation of the basic reproduction number (R0) for the novel coronavirus disease in Sri Lanka," *Virology Journal*, vol. 17, no. 1, p. 144, 2020.

[15] A. Omame, M. Abbas, and C. P. Onyenegecha, "A fractional-order model for COVID-19 and tuberculosis co-infection using Atangana–Baleanu derivative," *Chaos, Solitons and Fractals*, vol. 153, Article ID 111486, 2021.

[16] E. F. Doungmo Goufo, "Application of the Caputo–Fabrizio fractional derivative without singular kernel to Korteweg–de Vries–Burgers equation," *Mathematical Modelling and Analysis*, vol. 21, no. 2, pp. 188–198, 2016.

[17] M. Aslam, R. Murtaza, T. Abdeljawad et al., "A fractional order HIV/AIDS epidemic model with Mittag-Leffler kernel," *Advances in Differential Equations*, vol. 107, no. 1, p. 107, 2021.

[18] B. Karaagac and K. M. Owolabi, "Numerical analysis of polio model: a mathematical approach to epidemiological model using derivative with Mittag–Leffler Kernel," *Mathematical Methods in the Applied Sciences*, vol. 46, no. 7, pp. 8175–8192, 2021.

[19] A. Atangana, "Mathematical model of survival of fractional calculus, critics and their impact: how singular is our world?" *Advances in Differential Equations*, vol. 2021, no. 1, p. 403, 2021.

[20] G. Nazir, K. Shah, H. Alrabaiah, H. Khalil, and R. A. Khan, "Fractional dynamical analysis of measles spread model under vaccination corresponding to nonsingular fractional order derivative," *Advances in Differential Equations*, vol. 2020, no. 1, p. 171, 2020.

[21] Fatmawati, M. A. Khan, and H. P. Odinsyah, "Fractional model of HIV transmission with awareness effect," *Chaos, Solitons and Fractals*, vol. 138, pp. 109967–110779, 2020.

[22] B. H. Lichae, J. Biazar, and Z. Ayati, "The fractional differential model of HIV-1 infection of CD4+ T-cells with description of the effect of antiviral drug treatment," *Computational and Mathematical Methods in Medicine*, vol. 2019, Article ID 4059549, 12 pages, 2019.

[23] S. Rezapour, H. Mohammadi, and M. E. Samei, "SEIR epidemic model for COVID-19 transmission by Caputo derivative of fractional order," *Advances in Difference Equations*, vol. 2020, no. 1, p. 490, 2020.

[24] K. Rajagopal, N. Hasanzadeh, F. Parastesh, I. I. Hamarash, S. Jafari, and I. Hussain, "A fractional-order model for the novel coronavirus (COVID-19) outbreak," *Nonlinear Dynamics*, vol. 101, no. 1, pp. 711–718, 2020.

[25] M. A. Aba Oud, A. Ali, H. Alrabaiah, S. Ullah, M. A. Khan, and S. Islam, "A fractional order mathematical model for COVID-19 dynamics with quarantine, isolation, and environmental viral load," *Advances in Difference Equations*, vol. 1, no. 106, 2021.

[26] C. J Silva and D. F M Torres, "A TB-HIV/AIDS coinfection model and optimal control treatment," *Discrete and Continuous Dynamical Systems*, vol. 35, no. 9, pp. 4639–4663, 2015.

[27] I. Ullah, S. Ahmad, Q. Al-Mdallal, Z. A. Khan, H. Khan, and A. Khan, "Stability analysis of a dynamical model of tuberculosis with incomplete treatment," *Advances in Difference Equations*, vol. 2020, no. 1, p. 499, 2020.

[28] K. G. Mekonen, T. G. Habtemicheal, and S. F. Balcha, "Modeling the effect of contaminated objects for the transmission dynamics of COVID-19 pandemic with self protection behavior changes," *Results in Applied Mathematics*, vol. 9, Article ID 100134, 2021.

[29] A. I. K. Butt, W. Ahmad, M. Rafiq, and D. Baleanu, "Numerical analysis of Atangana-Baleanu fractional model to understand the propagation of a novel corona virus pandemic," *Alexandria Engineering Journal*, vol. 61, no. 9, pp. 7007–7027, 2022.

[30] K. Z. Zhang, N. A. Shah, D. Vieru, and E. R. El-Zahar, "Memory effects on conjugate buoyant convective transport of nanofluids in annular geometry: a generalized Cattaneo law of thermal flux," *International Communications in Heat and Mass Transfer*, vol. 135, Article ID 106138, 2022.